This is a repository copy of *(Si)GeSn nanostructures for light emitters*.

Proceedings Paper:

(Si)GeSn nanostructures for Light Emitters

D. Rainko*[a], D. Stange[a], N. von den Driesch[a], C. Schulte-Braucks[a], G. Mussler[a], Z. Ikonic[c], J.M. Hartmann[d], M. Luysberg[b], S. Mantl[a], D. Grützmacher[a] and D. Buca[a]

[a]Peter Grünberg Institute (PGI 9) and JARA – Fundamentals of Future Information Technologies, Forschungszentrum Juelich, Germany; [b]Peter Grünberg Institute (PGI 5) – Ernst Ruska Centre Juelich, Forschungszentrum Juelich, Germany; [c]Institute of Microwaves and Photonics, School of Electronic and Electrical Engineering, University of Leeds, United Kingdom; [d]CEA, LETI, MINATEC Campus and Univ. Grenoble Alpes, France

ABSTRACT

Energy-efficient integrated circuits for on-chip or chip-to-chip data transfer via photons could be tackled by monolithically grown group IV photonic devices. The major goal here is the realization of fully integrated group IV room temperature electrically driven lasers. An approach beyond the already demonstrated optically-pumped lasers would be the introduction of GeSn/(Si)Ge(Sn) heterostructures and exploitation of quantum mechanical effects by reducing the dimensionality, which affects the density of states. In this contribution we present epitaxial growth, processing and characterization of GeSn/(Si)Ge(Sn) heterostructures, ranging from GeSn/Ge multi quantum wells (MQWs) to GeSn quantum dots (QDs) embedded in a Ge matrix. Light emitting diodes (LEDs) were fabricated based on the MQW structure and structurally analyzed via TEM, XRD and RBS. Moreover, EL measurements were performed to investigate quantum confinement effects in the wells. The GeSn QDs were formed via Sn diffusion /segregation upon thermal annealing of GeSn single quantum wells (SQW) embedded in Ge layers. The evaluation of the experimental results is supported by band structure calculations of GeSn/(Si)Ge(Sn) heterostructures to investigate their applicability for photonic devices.

Keywords: GeSn, Direct bandgap, Optoelectronics, Silicon photonics, Group IV alloys, Light emitting diodes, Multi quantum wells, Quantum dots

1. INTRODUCTION

The concept of fully integrated light emitters on Si is a promising path towards energy-efficient electronic photonic integrated circuits (EPICs) due to their CMOS compatibility[1]. The main hindrance, however, is the absence of a direct bandgap in Si and Ge semiconductors, detrimental for efficient radiative recombination. Substitutional incorporation of Sn atoms and the introduction of tensile strain into the Ge lattice are two possible options to overcome this obstacle, leading to a fundamental direct bandgap in the Ge-based structure[2,3]. Lasing in a fundamental direct bandgap group IV GeSn alloy has already been demonstrated, making this material system very interesting for optoelectronic devices[3].

Cubic GeSn becomes a direct bandgap material for Sn concentrations above 9 at.%[3]. This transition is attributed to the effect that substitutional Sn atoms in the Ge lattice pull down the conduction band at the Γ point faster than that at L. Additionally, tensile strain enhances this tendency, while the compressive strain works against it[4,5].

While room temperature electroluminescence at low current densities from homojunction light emitting diodes (LEDs), relying on the direct band gap, has already been demonstrated[6–9], optically-pumped lasers still suffer from low maximum operating temperatures[3]. Those may be overcome by decreasing the residual compressive strain in the device by more elaborate geometries, like under-etched micro-disk resonators, or by using quantum effects in heterostructures, where

charge carriers are confined in a quantum well or a quantum dot[10,11,12]. Size-quantization effects influence both the recombination transition energy, i.e. the emitted wavelength, and also the density of states, which may lead to improvement of the lasing parameters, e.g. reduction of the threshold current density, as known from the history of III-V lasers[13].

Concerning GeSn active layers, obvious choices for barrier materials are Ge and SiGeSn due to their epitaxial compatibility. In this contribution, therefore, we will show temperature dependent light emission from compressively strained GeSn/Ge MQW LEDs with Sn concentrations around 8 at. %. In a more general discussion, we also investigate computationally the suitability of GeSn/Ge heterostructures in a range of strain conditions and compositions, and compare these with band alignment and barrier offsets achievable in GeSn/SiGeSn DHS. The formation of GeSn quantum dots (QDs) via annealing of compressively strained GeSn/Ge single QWs (SQW) with Sn concentrations of 10 at.% and their structural and optical characterization will also be discussed.

2. METHODS

a. Epitaxial growth and device processing

All (Si)GeSn/Ge heterostructures were grown using an industry-compatible AIXTRON reduced pressure CVD reactor on 200 mm Ge virtual substrates (Ge-VS) on Si(001) wafers. The growth temperature ranged between 365°C and 375°C. Both the dihydrides Ge_2H_6 and Si_2H_6, as well as $SnCl_4$ were used as precursor gases, which enable growth at low temperatures and allow the incorporation of large amounts of Sn[14]. For LED fabrication the active layers were sandwiched between p- and n-doped carrier injection GeSn layers.

Two different types of structures are discussed in this contribution, namely GeSn/Ge multi quantum well LEDs and undoped GeSn/Ge single quantum wells.

For the GeSn/Ge MQW LEDs, the p-doped GeSn bottom layers were grown above the critical thickness for strain relaxation, reducing the compressive strain in the GeSn QW subsequently grown. Moreover, the strain releasing dislocations are confined to the interface between the Ge-VS and the doped GeSn contact layer and guarantee a low defect density in the active region[6]. The GeSn/Ge MQW consists of several GeSn quantum wells, about 20 nm thick, separated by 14 nm Ge layers acting as barriers. The residual strain in the GeSn wells is -0.71% whereas the Ge barriers are tensely strained to +0.48%. On top of these layers, an n-doped GeSn layer was grown for electron injection into the active region.

The formation of the LEDs was performed using standard Si technology: reactive ion etching (RIE) of mesas using Cl_2/Ar plasma followed by the surface passivation by atomic layer deposition (ALD) of 10 nm Al_2O_3 at 300°C and subsequent plasma enhanced CVD (PECVD) of 150 nm SiO_2 at 300°C. After contact window opening via optical lithography and CHF_3 RIE, NiGeSn contacts were formed by sputtering of Ni and forming gas annealing at 325°C[15]. The last metallization step consists of 200 nm Al.

For the investigation of quantum dot formation, a GeSn layer with 10 at.% Sn and thickness of 17 nm was grown on top of a Ge-VS and capped by a 23 nm thick Ge layer. The samples went through different rapid thermal annealing processes in a temperature range between 400°C and 500°C under Ar ambient for 60 s and 120 s (see table 1).

Table 1. Experimental parameters for the RTP of GeSn SQW samples.

Sample	Annealing Temp. [°C]	Annealing time [s]
RTP_01	400	60
RTP_02	450	60
RTP_03	500	60
RTP_04	400	120
RTP_05	450	120
RTP_06	500	120

b. Structural characterization and electroluminescence measurements

Structural characterization of the LEDs was performed via Rutherford backscattering spectrometry (RBS), x-ray diffraction (XRD), transmission electron microscopy (TEM) and secondary ion mass spectrometry (SIMS). RBS spectra were measured using 1.4 MeV He$^+$ ions under 170° scattering angle, which gives information about stoichiometry, thickness and crystalline quality of the grown layers. X-ray diffraction reciprocal space mapping (XRD-RSM) measurements were performed using a Bruker D8 high-resolution diffractometer and the K$_\alpha$ wavelength of Cu around the (224) reflections. From these, the in- and out-of-plane lattice constants and, therefore, strain in the GeSn and Ge layers were identified. The sharpness of the interfaces and the distribution of doping elements was analyzed by TEM and SIMS. For TEM measurements the cross sectional specimens have been prepared by grinding and Ar ion milling. Investigations of the structural properties and local composition were performed with FEI Tecnai F20 and FEI Titan 80-200 equipped with Super X EDX detector, respectively.

Light emission from the MQW LEDs as well as from the annealed GeSn QDs was studied with a Bruker VERTEX 80 V FTIR spectrometer in step scan mode. Spectra were recorded in a temperature range between 4 K and room temperature (300 K) using a liquid He cold finger, on which the samples were mounted. The samples were excited by 2 kHz pulses with 50% duty cycle, and the emitted luminescence was detected by a nitrogen-cooled InSb detector, while a cut-off filter at around 3 µm ensured a minimized influence of thermal radiation.

c. Numerical calculations

The band structure and alignment of heterostructures, including the GeSn/Ge MQW, as well as the bulk materials were also investigated computationally, with the structural parameters coming from the layer's structural characterization. The band energies of the bulk material were calculated using the deformation potentials, and 8x8 k·p method including strain effects, with the parameters of Si, Ge and Sn taken from literature[16,17]. Concerning the quantum well structures, quantization energies were calculated using the effective mass method for electrons in L and Γ bands, and the 6x6 k·p method for LH, HH and SO bands.

3. RESULTS AND DISCUSSION

The MQW LED is schematically shown in Figure 1 together with structural characterization by TEM, RBS and XRD. Cross-sectional TEM (XTEM) micrographs (inset in Fig. 1a) show sharp interfaces between Ge barriers and GeSn wells. Moreover, a high concentration of threading dislocations at the GeSn:P/Ge interface without propagation into the MQW region were found. This indicates a partial relaxation of the doped GeSn:P buffer layer, which reduces the compressive strain in the GeSn wells. To investigate the crystal quality of the layer structure RBS measurements have been performed, at which the MQW structure was either aligned randomly to the 1.4 MeV He$^+$ beam, or along the lattice channeling direction. The ratio between the number of scattered ions in channeling and random measurements χ_{min}, determined behind the surface peak, is correlated with the atom substitutionality in the investigated layer. The minimum channeling yield of 6% evidences a high crystal quality with large substitution of Sn atoms in the Ge lattice (Figure 1 (b)). Figure 1 (c) shows RSM measurements, where the periodicity of the MQW as well as the reflection coming from the p-doped GeSn buffer and the Ge-VS are visible. Strain values of -0.71% and +0.48% are extracted for the GeSn wells and Ge barriers, respectively. The dashed line in Figure 1 (c) shows that the complete MQW has the same in-plane lattice constant as the partially relaxed p-doped GeSn buffer, meaning that it is pseudomorphically grown on top of the GeSn buffer. The partial relaxation of the buffer is also indicated by the reflection from the Ge-VS, which is not aligned with the reflection from the overgrown structure.
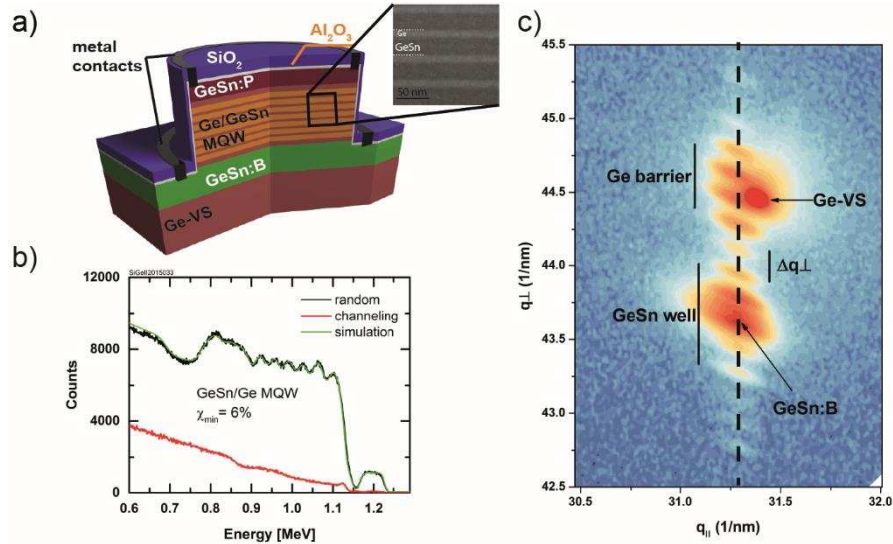
Figure 1. (a) Device design of the MQW LED with XTEM micrograph of the GeSn/Ge MQW as inset. (b) RBS spectrum revealing high crystal quality with a χ_{min} of 6%. (c) XRD reciprocal space map image of the MQW to identify the in-plane and out-of-plane lattice constants of the layer structure.

Figure 2 (a) shows EL spectra at a current density of 420 A/cm² for temperatures between 4 and 300 K of the GeSn/Ge MQW. The emission peak centered at 0.6 eV (at 300 K) shifts about 20 meV at 4 K, due to the temperature dependence of the bandgap. The calculated electronic band structure of the MQW (Figure 2 (b)) reveals a weak carrier confinement. It indicates that both GeSn and the Ge barriers are indirect semiconductors, the L-band energy lies below the Γ-band energy. More important from the carrier confinement point of view, Type I alignment is not achieved for electrons. The GeSn "well" serves as a quantum well only for holes, but not for L electrons; those are actually confined within the Ge barrier. In conclusion, the interplay between compressive strain in the well and tensile strain in the barrier cause only a small band offset in the conduction band and, therefore, poor carrier confinement.
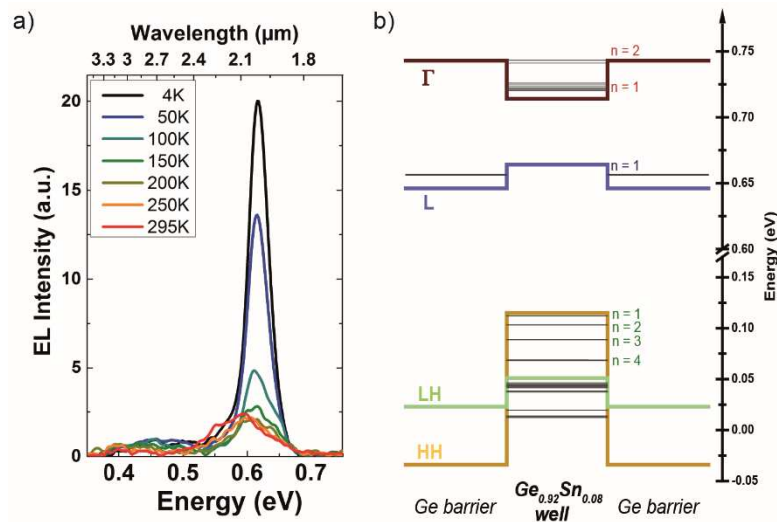

Figure 2. (a) Temperature dependent EL spectra of the GeSn/Ge MQW. (b) Band structure calculations based on the thickness, stoichiometry and strain information of the MQW.

In order to get a more general idea on which layer composition creates a band structure suitable for efficient light emission, calculations have been performed for pseudomorphically grown GeSn/Ge layers on fully relaxed GeSn buffer (Figure 3 (a)). The Sn concentration of both the buffer and top GeSn well were varied in the range 0 – at.%, which is experimentally accessible in epitaxial growth[14]. In recent publications we have examined the region where the GeSn well undergoes a

transition from indirect to direct bandgap depending on the Sn concentration in the GeSn buffer and well[6,18]. If we exclude the parameter configurations in which the GeSn well has an indirect, the Ge well has a direct bandgap and where the alignment for the Γ bands is not of type I, only a small parameter space is left, suitable for carrier confinement (green area, Figure 3 (b)). The DHS in this region should exhibit a high offset between the well and the barrier in comparison to the thermal energy at 300 K for application in efficient light emitters. In Figure 3 (c) the barrier heights for Γ-electrons, in units of $k_B T$ at 300 K, are plotted for different Sn concentrations in the GeSn buffer and well. In this regime only low barrier heights with a maximum of only ~1.5 $k_B T$ can be obtained, so that the material system GeSn/Ge can be excluded as an efficient group IV heterostructure for light emitters.
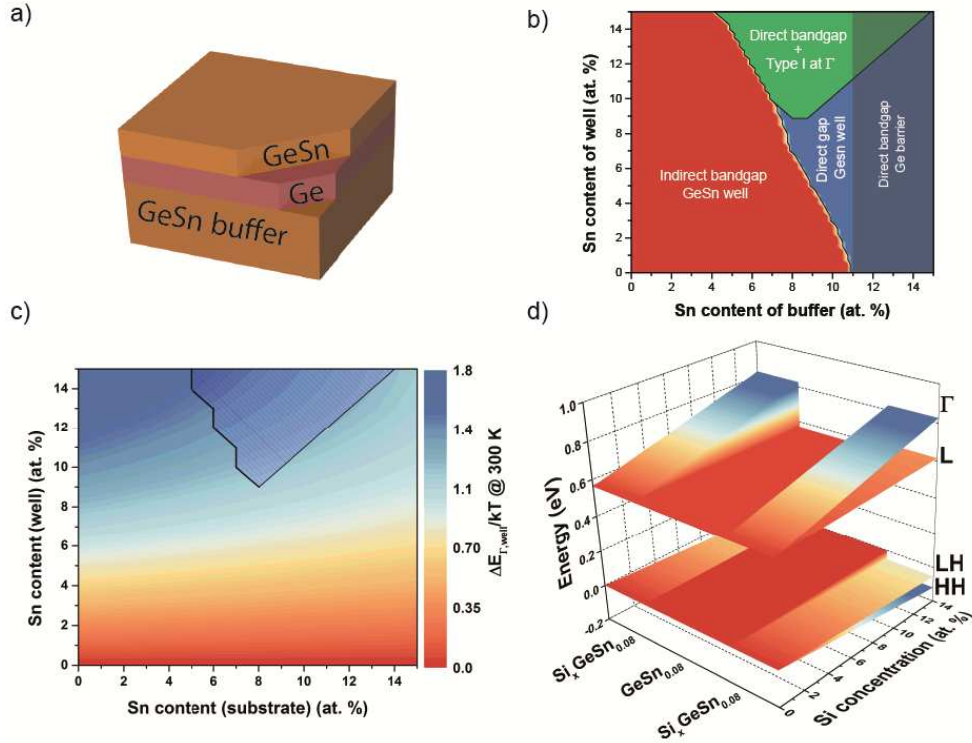

Figure 3. (a) Layer structure of GeSn/Ge DHS. (b) Regions where the GeSn well of the structure has a direct/indirect bandgap (blue/red area), where the Ge barrier becomes a direct bandgap (shaded area), and where the alignment of barrier and well is type I (green area). (c) Γ band barrier heights relative to $k_B T$ @ 300 K for the green area of (b). (d) Band profile of a GeSn$_{0.08}$/Si$_x$GeSn$_{0.08}$ DHS.

SiGeSn is a more suitable barrier material for carrier confinement in GeSn heterostructures[6,19]. Figure 3 (d) shows band profiles of GeSn/SiGeSn double heterostructures (DHS), where bulk GeSn with Sn concentration of around 8 at.% is deposited in between two SiGeSn layers with a Si concentration varying between 1 and 14 at.% and a fixed Sn concentration of 8 at.%. The SiGeSn barriers are indirect alloys while the GeSn well is direct. Type I alignment, with band offsets up to 263 meV for the Γ band edges and 47 meV for the L bands, is here possible. These results indicate the prospects of using GeSn/SiGeSn heterostructure configurations for efficient GeSn LEDs and LDs.

Another type of structure, which modifies the material properties, are quantum dots embedded in a crystalline matrix. With sufficiently small sizes of QDs one can get well separated discrete bounded states with a 0D type of density of states. By changing the dot size an additional tuning of bandgap and, therefore, of the emitted wavelength is possible. These structures are very interesting for photonic applications, in particular for detector and laser applications[20,21].

There are several ways to create QDs, from direct over-growth on template substrates to controlled diffusion and segregation[22,23]. The low solubility of Sn in Ge can be used for QDs formation by simply annealing the GeSn layers, which causes the precipitation of Sn[24]. Following this approach to form GeSn QDs we grew Ge/GeSn/Ge single quantum wells (SQW), as depicted in Figure 4 (a), before performing rapid thermal annealing at temperatures between 400°C and 500°C to create Ge$_{1-x}$Sn$_x$ precipitations in the bulk material (Table 1). The untreated SQW shows a high crystal quality, with a

channeling minimum yield χ_{min} of 4.5% (Figure 4 (b)), while TEM micrographs show sharp interfaces without misfit dislocations (Figure 4 (c)). All annealed samples show quantum dot formation within the initial GeSn well (Figure 4 (d)). The occurrence of Moiré patterns on XTEM micrographs indicate their crystallinity, and also reveal the fact that the dots are not coherently oriented to the surrounding Ge lattice.
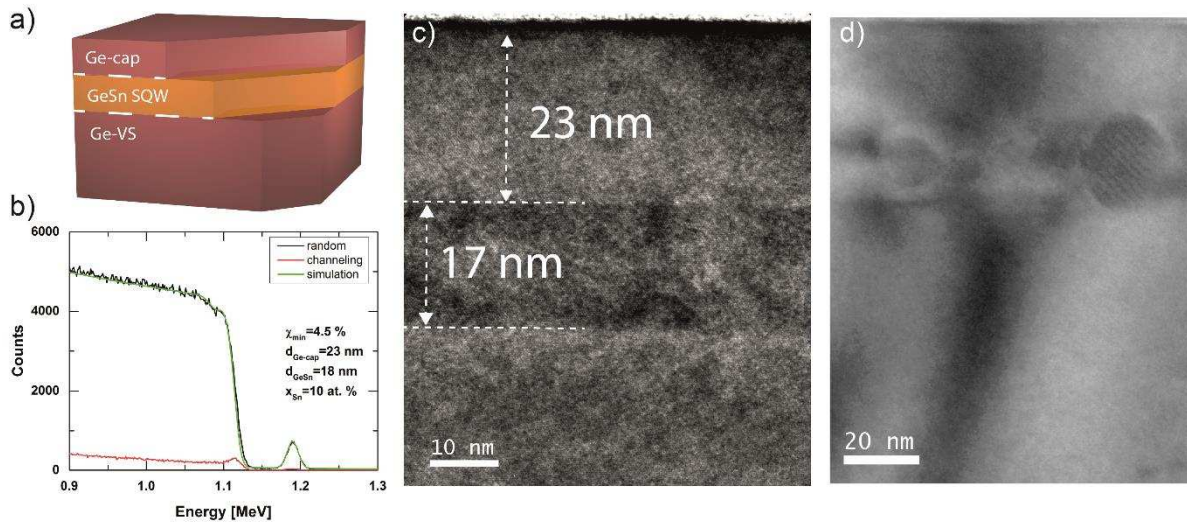

Figure 4. (a) Layer structure of the GeSn SQW surrounded by Ge layers. (b) RBS spectrum of the SQW indicating a high crystal quality. (c) XTEM micrograph showing the GeSn well and Ge barriers. (d) $Ge_{1-x}Sn_x$ precipitates inside of the GeSn well after the annealing process.

To acquire more information about the GeSn dots, energy dispersive x-ray spectroscopy (EDX) mapping was performed. Figure 5 (a) shows a high angle annular dark field micrograph (HAADF) where heavier elements i.e. Sn produce brighter contrast. The corresponding EDX map of the Ge and Sn absorption edges are displayed in Figure 5 (b). Clearly, an increased amount of Sn is revealed inside the dots indicating that they were created due to precipitation of Sn inside the SQW (Figure 5 (b)). However, the absolute Sn concentration cannot be derived from this measurement, since the surrounding matrix obscures the detection of the EDX signals stemming solely from the QDs. Further experiments are needed for evaluation of Sn content as well as the crystal structure.
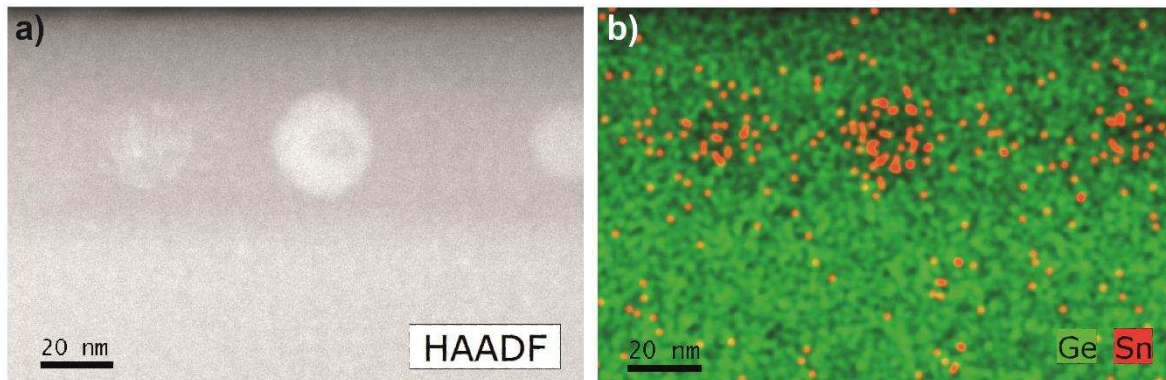

Figure 5. (a, b) HAADF micrograph of several $Ge_{1-x}Sn_x$ precipitates and the corresponding EDX maps of Ge and Sn.

PL measurements on the as-grown and annealed SQWs have been performed and are shown in (Figure 6). The spectra of the as-grown SQW show three distinct peaks at energies of ~0.5 eV, ~0.59 eV and ~0.43 eV. From band structure calculations the first two may be associated with transition from Γ and L, respectively, to the heavy hole band. The last peak, since positioned below the bandgap, may be ascribed to defects[4]. After the annealing process only one peak, at about 0.48 eV is visible. Moreover, the peak position is at a lower energy, indicating a lower effective band gap. Band structure calculations for unstrained $Ge_{0.9}Sn_{0.1}$ SQW indicate a bandgap of ~0.51 eV, which would even increase if the Sn

concentration decreases due to the precipitation of Sn. Therefore this PL emission peak cannot directly be attributed to the strain relaxation of the initial GeSn layer. In the formed QD the Sn content is expected to be higher and the competition between high Sn content and compressive strain may lead to emission at lower energies. Nevertheless, no radiative transitions can be exactly attributed to the quantum dots. Further experiments and calculations will provide more evidence on the compositional and electronic properties of these precipitates.
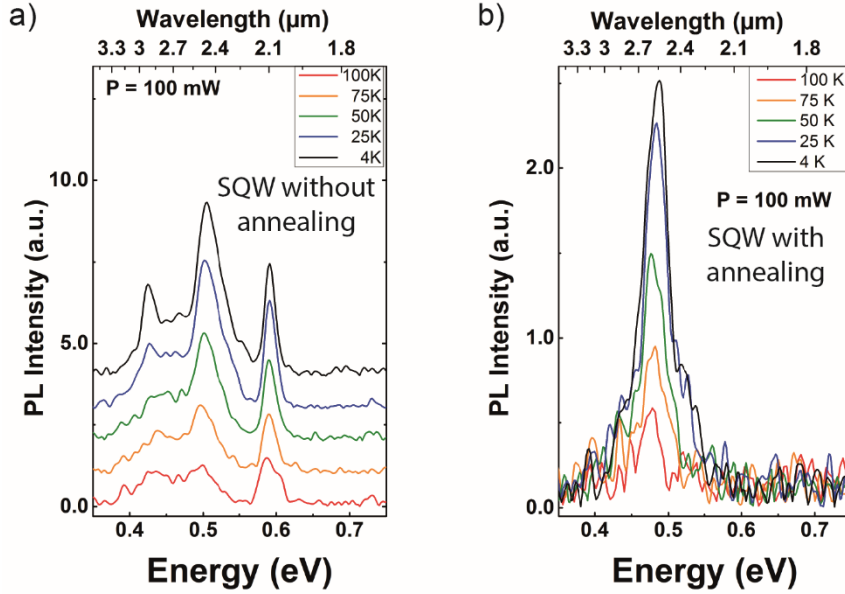

Figure 6. Temperature dependent PL spectra of the as-grown GeSn SQW (a) and an annealed sample with quantum dots (b).

4. SUMMARY AND OUTLOOK

In this contribution we present growth and characterization of GeSn MQW and SQWs embedded in a Ge matrix. Structural characterizations of the MQW device reveal a structure with sharp layer boundaries and high crystal quality. EL spectra could be measured in the temperature range between 4 and 300 K. The k·p and effective mass method calculations show a generally weak carrier confinement in GeSn/Ge heterostructures. Furthermore, the parameter space for type I alignment with epitaxially reasonable Sn concentrations is very small, making GeSn/Ge heterostructures unsuitable for efficient light emitters. SiGeSn is introduced as barrier material, where band structure calculations show much larger barrier heights, predicting a more efficient carrier confinement of charge carriers in the conduction band.

Finally, formation of GeSn quantum dots is demonstrated, with precipitation of Sn inside the GeSn SQWs. From mapping analysis an increased amount of Sn could be measured. However, PL measurements do not reveal any radiative transitions originating in the QDs. Still, a more detailed investigation of composition and electronic structure of GeSn QDs will be necessary.

REFERENCES

[1]   Soref, R., "Mid-infrared photonics in silicon and germanium," Nat. Photonics **4**(8), 495–497 (2010).

[2]   Süess, M. J., Geiger, R., Minamisawa, R. A., Schiefler, G., Frigerio, J., Chrastina, D., Isella, G., Spolenak, R., Faist, J., et al., "Analysis of enhanced light emission from highly strained germanium microbridges," Nat. Photonics **7**(6), 466–472 (2013).

[3]   Wirths, S., Geiger, R., von den Driesch, N., Mussler, G., Stoica, T., Mantl, S., Ikonic, Z., Luysberg, M., Chiussi, S., et al., "Lasing in direct-bandgap GeSn alloy grown on Si," Nat. Photonics **9**(2), 88–92 (2015).

[4]   Stange, D., Wirths, S., von den Driesch, N., Mussler, G., Stoica, T., Ikonic, Z., Hartmann, J. M., Mantl, S., Grützmacher, D., et al., "Optical Transitions in Direct-Bandgap Ge1-xSnx Alloys," ACS Photonics **2**(11), 1539–1545 (2015).

[5]   Gupta, S., Magyari-Köpe, B., Nishi, Y.., Saraswat, K. C., "Achieving direct band gap in germanium through integration of Sn alloying and external strain," J. Appl. Phys. **113**(7), 073707 (2013).

[6]   Stange, D., von den Driesch, N., Rainko, D., Schulte-Braucks, C., Wirths, S., Mussler, G., Tiedemann, A. T., Stoica, T., Hartmann, J. M., et al., "Study of GeSn based heterostructures: towards optimized group IV MQW LEDs," Opt. Express **24**(2), 1358 (2016).

[7]   Gallagher, J. D., Senaratne, C. L., Xu, C., Sims, P., Aoki, T., Smith, D. J., Menéndez, J.., Kouvetakis, J., "Non-radiative recombination in Ge1−ySny light emitting diodes: The role of strain relaxation in tuned heterostructure designs," J. Appl. Phys. **117**(24), 245704 (2015).

[8]   Koerner, R., Oehme, M., Gollhofer, M., Schmid, M., Kostecki, K., Bechler, S., Widmann, D., Kasper, E.., Schulze, J., "Electrically pumped lasing from Ge Fabry-Perot resonators on Si," Opt. Express **23**(11), 14815 (2015).

[9]   Oehme, M., Werner, J., Gollhofer, M., Schmid, M., Kaschel, M., Kasper, E.., Schulze, J., "Room Temperature Electroluminescence from GeSn Light Emitting pin Diodes on Si (August 2011)," IEEE Photonics Technol. Lett. **23**(23), 1751–1753 (2011).

[10]   Soref, R. A., "Direct-gap Ge/GeSn/Si and GeSn/Ge/Si heterostructures," Superlattices Microstruct. **14**(2/3), 189–193 (1994).

[11]   Chen, R., Gupta, S., Huang, Y. C., Huo, Y., Rudy, C. W., Sanchez, E., Kim, Y., Kamins, T. I., Saraswat, K. C., et al., "Demonstration of a Ge/GeSn/Ge quantum-well microdisk resonator on silicon: Enabling high-quality Ge(Sn) materials for micro-and nanophotonics," Nano Lett. **14**(1), 37–43 (2014).

[12]   Ferry, D. K., "The onset of quantization in ultra-submicron semiconductor devices," Superlattices Microstruct. **27**(2-3), 61–66 (2000).

[13]   Alferov, Z., "Double heterostructure lasers: Early days and future perspectives," IEEE J. Sel. Top. Quantum Electron. **6**(6), 832–840 (2000).

[14]   von den Driesch, N., Stange, D., Wirths, S., Mussler, G., Holländer, B., Ikonic, Z., Hartmann, J. M., Stoica, T., Mantl, S., et al., "Direct Bandgap Group IV Epitaxy on Si for Laser Applications," Chem. Mater. **27**, 4693–4702 (2015).

[15]   Wirths, S., Troitsch, R., Mussler, G., Zaumseil, P., Hartmann, J. M., Schroeder, T., Mantl, S.., Buca, D., "Ni(SiGeSn) Metal Contact Formation on Low Bandgap Strained (Si)Ge(Sn) Semiconductors," ECS Trans. **64**(6), 107–112 (2014).

[16]   Wirths, S., Geiger, R., von den Driesch, N., Mussler, G., Stoica, T., Mantl, S., Ikonic, Z., Luysberg, M., Chiussi, S., et al., "Lasing in direct-bandgap GeSn alloy grown on Si - Supplementary Information," Nat. Photonics **9**(2), 88–92 (2015).

[17]   Bahder, T. B., "Eight-band kp model of strained zinc-blende crystals," Phys. Rev. B **41**(17), 11992–12001 (1990).

[18]   von den Driesch, N., Stange, D., Wirths, S., Rainko, D., Mussler, G.., Grützmacher, P., "Direct bandgap GeSn light emitting diodes for short-wave infrared applications grown on Si," SPIE Photonics West (2016).

[19]   Sun, G., Soref, R. A.., Cheng, H. H., "Design of an electrically pumped SiGeSn/GeSn/SiGeSn double-heterostructure midinfrared laser," J. Appl. Phys. **108**(3) (2010).

[20]   Alivisatos, A. P., "Semiconductor Clusters, Nanocrystals, and Quantum Dots," Science (80-.). **271**(5251), 933–937 (1996).

[21]   Klimov, V. I., Mikhailovsky, A., Xu, S., Malko, A., Hollingsworth, J., Leatherdale, C., Eisler, H.., Bawendi, M. G., "Optical Gain and Stimulated Emission in Nanocrystal Quantum Dots," Science (80-.). **290**(5490), 314–317 (2000).

[22]   Roesgaard, S., Chevallier, J., Gaiduk, P. I., Hansen, J. L., Jensen, P. B., Larsen, A. N., Svane, A., Balling, P.., Julsgaard, B., "Light emission from silicon with tin-containing nanocrystals," AIP Adv. **5**(7) (2015).

[23]   Leonard, D., Krishnamurthy, M., Reaves, C. M., Denbaars, S. P.., Petroff, P. M., "Direct formation of quantum-sized dots from uniform coherent islands of InGaAs on GaAs surfaces," Appl. Phys. Lett. **63**(23), 3203–3205 (1993).

[24]   Tonkikh, A., Zakharov, N. D., Suvorova, A., Eisenschmidt, C., Schilling, J.., Werner, P., "Cubic phase Sn-rich GeSn nanocrystals in a Ge matrix," Cryst. Growth Des. **14**(4), 1617–1622 (2014).